

RAMAN SPECTROSCOPY TECHNIQUES AND TECHNOLOGY AS A TOOL IN ENVIRONMENTAL WATER ANALYSIS

KARLO MAŠKARIĆ^{1,2,3}, SIMONA CÎNTĂ PÎNZARU^{1,2,*}, DĂNUȚ-ALEXANDRU DUMITRU^{1,2}, CSILLA MOLNAR⁴, DRÎGLĂ TEODORA DIANA¹, SANJA TOMŠIĆ³, ANA BRATOȘ CETINIĆ³

DOI: 10.24193/AWC2024_12

ABSTRACT. Raman Spectroscopy Techniques and Technology as a Tool in Environmental Water Analysis. Although the normal Raman scattering effect is inherently weak in diluted solutions such as environmental waters and dedicated enhancing techniques are already suitable for trace analysis of many harmful compounds, pollutants, toxins, and other species from aquatic environments, here we demonstrate how Raman spectroscopy techniques and technology can be effectively applied for environmental water analysis. Usually, normal Raman spectra of environmental waters, such as seawater, salt lakes waters show a weak-medium sulfate signal at about 981 cm^{-1} along with the stretching and bending modes of water. Rarely, weak bands attributable to dissolved CO_2 and HCO_3^- are visible with weak intensity. We compared NIR-Raman and Raman spectra with visible laser excitation at 532 nm, which is resonant for carotenoids-containing microorganisms from water in bulk liquid or drop coating deposition samples, in multiple water samples from different spatial and temporal locations to include seawaters from Adriatic Sea (oligotrophic), Black Sea (eutrophic) and salt lakes waters (Cojocna Lakes (Lake1 and Lake2), Ursu Lake, Dead Sea). Valuable information can be obtained by combining resonance Raman spectroscopy using a Renishaw InVia Raman system coupled with a Leica research-grade microscope with a 532 nm laser with information from the FT-Raman spectra of the same waters. When photosynthetic microorganisms are abundant, in non-resonance conditions, a weak band of carotenoids is visible in FT-Raman or NIR-Raman spectra, suggesting photosynthetic microorganisms abundance. Such bulk waters show a high fluorescence background that sometimes covers any band, or reveal resonantly-enhance carotenoid bands arising from microorganisms under 532 nm excitation when Raman spectra of bulk liquid are tried. Drop coating deposition Raman (DCDR) technique could be more effective in rapidly assessing water droplet content under confocal micro-Raman spectroscopy. Both FT-Raman and microscopy techniques always record the sulfate ν_1 (SO_4^{2-}) Raman band at $\sim 981\text{ cm}^{-1}$ and water bands, $\delta(\text{OH})$ at $\sim 1637\text{ cm}^{-1}$ and $\nu(\text{OH})$ Raman band at $\sim 3218\text{ cm}^{-1}$ as shown in several comparative examples. Relative intensity ratio of $\sim 981\text{ cm}^{-1}$ and

¹Babeș-Bolyai University, Biomolecular Physics Department, Kogălniceanu 1, RO-400084, Cluj Napoca, Romania; karlo.maskaric@ubbcluj.ro; simona.pinzaru@ubbcluj.ro, danut.dumitru@stud.ubbcluj.ro, teodoradrigla@yahoo.com

²Institute for Research, Development and Innovation in Applied Natural Sciences, Babes-Bolyai University, Fantanele 30, Cluj-Napoca, Romania;

³Department of Applied Ecology, University of Dubrovnik, Ćira Carića 4, 20 000 Dubrovnik, Croatia; sanja.tomsic@unidu.hr; abratos@unidu.hr

⁴National Institute for Research and Development of Isotopic and Molecular Technologies, 67-103 Donath, 400293 Cluj-Napoca, Romania; csilla.molnar@itim-cj.ro.

$\sim 1637\text{ cm}^{-1}$ is proportional to sulfate concentration and can be used for quantitative sulfate analysis, based on an adequate calibration curve of sulfate solutions. Two sample tests for variance (F-test) revealed significant differences between relative intensity ratio between the Black Sea and Adriatic Sea samples when $p < 0.05$. SO_4^{2-} concentration variation is accompanied by other ion concentration variations and, thus, linked with salinity, conductivity and pH, which are related to climate events, and also influence the distribution of aquatic organisms. Thus, combined Raman spectroscopy techniques and technology for environmental water measurements can provide fast and useful information for monitoring programs and highlight large differences between oligotrophic and eutrophic seawaters or salt lakes and their spatial-temporal dynamic change.

Keywords: FT-Raman, relative intensity ratio, environmental water monitoring, Adriatic Sea, Black Sea

1. INTRODUCTION

Environmental water bodies such as seawater or salt lakes raise increasing concern regarding their chemical content and fluctuations which affect the economy and ecosystem (Kumar et al., 2024). Raman spectroscopy techniques and methods have been employed for various topics, such as water monitoring programs, harmful chemicals detection, microplastic contamination, algal blooms, and others (Kniggendorf et al., 2019, Li et al., 2014, Ong et al., 2020, Zhao et al., 2023). We argue regular Raman spectroscopy could give relevant information for chemical water analysis, a concept supported by the combined use of similar other spectroscopic techniques employed by others (Bao et al., 2022, Fan et al., 2022). Especially in this case for estimating sulfate (SO_4^{2-}) ion concentration and monitoring its fluctuation. Recently, in our group we demonstrated that in saltwater bodies such as hypersaline lakes (Molnar et al, 2023), sulfate content provides a ubiquitous Raman signal of waters, which is visible under any experimental conditions, even for 1 s Raman spectral acquisition. Moreover, the sulfate band intensity observed in the $979\text{-}981\text{ cm}^{-1}$ range is positively correlated with the classical parameters which are usually investigated in comprehensive physicochemical approaches which include the electrical conductivity, pH, and total dissolved solids (Molnar et al, 2023). Raman quantification can sometimes be difficult to get right, and we understand the frustrations these challenges can bring, particularly to non-spectroscopists, aiming to use Raman technology for environmental waters. Because of these issues, we show in Fig 1. the origin of errors, when a linear calibration curve is built for quantitative Raman measurements of aqueous sulfate solutions. These challenges are particularly pronounced when dealing small amounts of liquid solutions, aiming for the target technique to be fast, in terms of short acquisition time (in many cases, 1 s preferred), to adapt the requirements for environmental applications. Technical methodology to build reliable calibration curves for quantitative determination of certain chemical content in environmental waters has to take into account the inherently weak Raman signal of diluted solutions, the solvent effects, conditions, the co-existence of other natural ingredients, both organic and inorganic (Bao et al., 2022) and to design specific strategy

for targeting certain compounds and combine with enhancement techniques, such as resonance Raman (when applied) or surface-enhanced Raman techniques. Based on these recent results, we conducted a comparative investigation of several saltwater bodies, exploring the discrimination of water samples solely relating to the normal Raman signal of raw samples, without any chemical treatment or extraction.

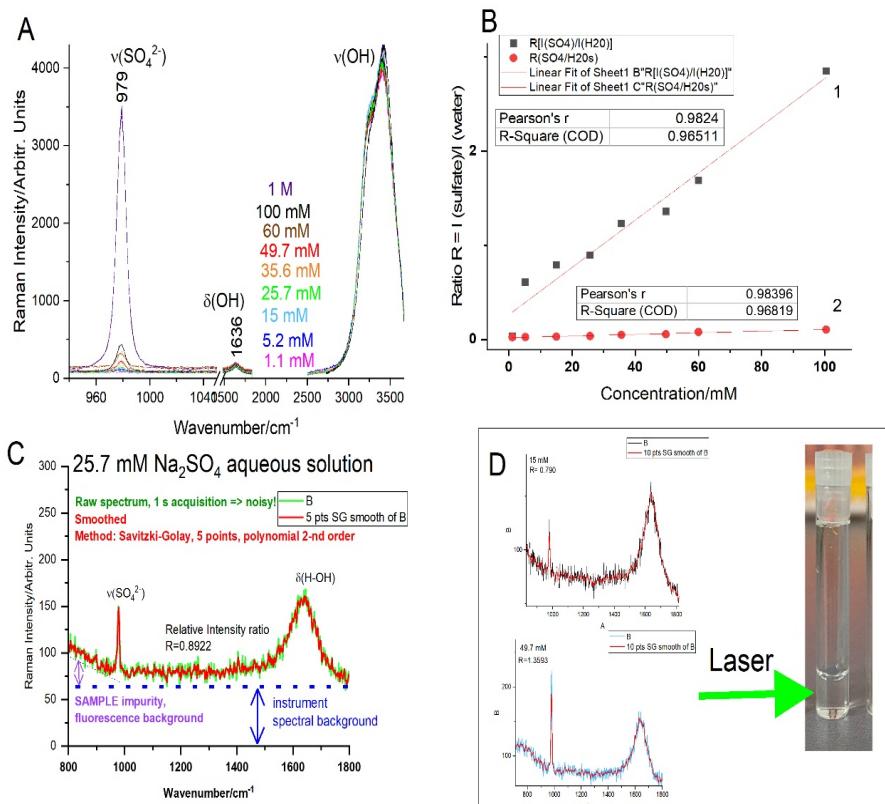


Figure 1. **A**) The Raman spectra of sodium sulfate aqueous solutions of various concentrations, from 1.1 mM to 1M, as indicated; **B**) The two calibration curves (1, 2) against concentration with a linear fit ($r^2=0.96$) obtained by calculating Raman intensity ratios of sulfate at 979 cm^{-1} to water bending mode at 1636 cm^{-1} (1) or to stretching symmetric mode at 3242 cm^{-1} , (2), for 1 s Raman acquisition; **C**) The raw Raman spectrum of a sulfate solution of 25.7 mM, illustrating the sources of errors by ignoring the instrument background correction of spectra and the smoothing to reduce noise for 1 s acquisition; and **D**) A typical sampling approach of the small liquid sample and two raw spectra of aqueous sulfate of 15 and 40.7 mM, superimposed with their smoothed version, with clearly reduced sulfate band intensity.

The two values (15 and 40.7 mM) defined a sufficiently large concentration interval to include the current averaged ocean concentration (28 mM) and to illustrate that sulfate band intensity is comparable with the water bending mode intensity. For the calibration curves in **B**) the background corrections and smoothing were not applied; an averaged signal of three independent measurements was used to reduce noise. Excitation: 532 nm, 1 s acquisition.

2. EXPERIMENTAL

2. 1. **Sampling** has been achieved by collecting either surface waters (0.2-1 m depth) from two adjacent hypersaline lakes of Cojocna Balneary Resort (Cluj County, Romania) in October 2023, Ursu Lake (Mures County, Romania) and the Dead Sea shore (North Western point, Kalia Beach, September 2023). In addition were collected the surface and depth waters from the Western side of the Black Sea (Passarella Mamaia, April 2018; Constanta, January 2023- surface waters) or water column samples taken with a CTD SBE 25 Sea logger at cca. 100 km offshore of Constanta, from depths varying from 0 to 30 m (March 2019). Other 10 locations on the South Adriatic Sea coast of Croatia were sampled in 2014 and 2015 every month from 1 m depth, including Dubrovnik Old Port offshore, Gruz Gulf (East and West), Lapad Gulf, Kalamota Island coast, Makarska (North and South), Mlini, Cavtat and Ston (aquaculture area). Additionally, one depth profile comprising seawater samples from 0.5, 5, 10, 15, and 20 m depth has been taken offshore of Dubrovnik, heading Lokrum Island (February 2015). Samples were taken using a Niskin bottle device and transferred to a 0.5 l bottle for lab measurements in the next 24 hours from each collection.

2. 2. Equipment. FT-Raman spectra of waters in a 2 ml quartz cuvette with a cap have been recorded with an Equinox 55 FT-IR Bruker Spectrometer with an integrated FRA106S Raman module. A Nd:YAG laser line at 1064 nm was employed for excitation (350-mW output power). Detection was achieved with a nitrogen-cooled Ge detector. Spectral resolution was 4 cm^{-1} and 500 scans were set in Opus 2.0 software.

Normal Raman spectra of bulk samples excited with a 532 nm laser line was measured with Renishaw InVia Reflex Raman system with a RenCam CCD detector, 1024x256 pixels (200-1060 nm) using a liquid holder accessory, 1 s exposure, 1 acquisition, and 100% laser power (200 mW) set in Wire 3.4 acquisition software.

For drop-coating deposition Raman (DCDR) a hydrophobic stainless steel μ -rim slide has been used to deposit spherical water droplets of 5 μl and measured immediately using the Leica inViaTM research-grade confocal Raman microscope with 5x objective, with spectral resolution 0.5 cm^{-1} under 532 nm line excitation. Short acquisitions of 1 s were applied to rapidly record the spectra in the 50-1800 cm^{-1} range. Besides short acquisition, extended acquisition of 10 min was performed on the samples in the 100-3000 cm^{-1} range.

2. 3. Data analysis and methods. A comparison of seawater and salt lake waters spectra was done on 10 samples collected from the South Adriatic Sea Coast, one sample from the Black Sea, one from the Ursu Lake, and one-one sample from each of Cojocna lakes.. Further, 42 samples from the Black Sea are presented to show spatial variations of sulfate band intensity at different locations from Passarella Mamaia (April 2018 and different depth in the water column from Constanța (March 2019). Moreover, 43 samples from the Adriatic Sea are presented in time dependence series to comprise waters from the same locations, with emphasis on comparing differences in sulfate level in aquaculture area (Ston) with open sea, not used for aquaculture. Drop-coated deposition samples were from the Adriatic Sea, Black Sea, Dead Sea and two Cojocna lakes. Samples from the Adriatic Sea, Black Sea and Dead Sea were acquired in both extended and normal acquisition. Black Sea data (Constanța January 2023) of concentrated seawater with abundant microorganisms shown as a case of resonant Raman spectra. Taking into account errors that could arise from the relative intensity ratio calculations, sample averages from two Cojocna lakes (11 subsamples each lake, October 2023) were presented including error bars based on a standard deviation of mean values from each lake. OriginPro 2021b software was used for plotting graphs and columns, and for statistical analysis.

3. RESULTS AND DISCUSSION

All the FT-Raman spectra of water showed the sulfate stretching mode band at 979 cm^{-1} and the characteristic water vibrational modes, at 1637 cm^{-1} (bending) and water stretching modes at 3235 cm^{-1} (Fig 2., Fig 3., Fig 4.). Regarding the comparison of different water bodies, the highest relative intensity ratio of sulfate to water band was recorded in the Adriatic Sea in December 2017 (Fig 2. A, B).

Two sample test for variance (F-test) revealed a significant difference between the relative intensity ratio between the Black Sea and the Adriatic Sea samples, when $p < 0.05$ (Fig 3., Fig 4.). F test revealed no significant difference between relative intensity ratio of surface and depth waters from the Black Sea, when $p < 0.05$ (Fig 3.). The F test found no significant differences between values of aquaculture and areas not used for aquaculture during 2014 in the Adriatic Sea (Fig 4. A, B). However, the same test found a significant difference in the same case during 2015 (Fig 4. C, D). Depth profile variations was significantly different from the surface waters (F-test, $p < 0.05$) for the Adriatic Sea samples from 2015 (Fig. 4). Relative intensity ratio of sulfate to water bands were significantly different between 2014 and 2015 in the investigated area of the Adriatic Sea (Fig 4). Furthermore, according to the one sample T test at $p < 0.05$ level, both the Adriatic Sea and the Black Sea significantly differ from the standard ocean value of the sulfate level, which is 28 mM (Zhu et al., 2021). DCDR with 532 nm laser excitation samples of every body of water recorded sulfate stretching band 979 cm^{-1} and water bending band 1637 cm^{-1} (Fig 5., Fig 6.). Spectra of shorter acquisition time; Adriatic Sea and Dead Sea (Fig 5.) have clearer but lower intensity bands of sulfate and water compared to other spectra. The same samples under extended acquisition range and longer time (10 minutes) have a higher background, but nevertheless clear sulfate and water bands (Fig 5.). Both the short-time acquisition and extended range longer acquisition spectra from the Black Sea have higher background in comparison with the samples from the Adriatic Sea and Dead Sea, their sulfate and water bands were less prominent (Fig 5.). Depending on the acquisition time, the intensity band of sulfate and water change. This fact could be attributed to the water heating (Bao et al., 2022), which results in different intensity values for sulfate and water, ergo the relative ratio for the same sample is different. One of the Cojocna lake spectra has weak bands at 1288 cm^{-1} and 1388 cm^{-1} (Fig 5.). These bands can be attributed to CO_2 (Shirmohammad et al., 2023). The average relative intensity ratio of 11 spectra from each of the Cojocna lakes (October 2023) is different (Fig 6. A, B). One spectrum from one of the lakes had bands characteristic for carotenoids (Fig 6. A) due to microorganisms present in the lake (Molnár et al., 2023). Concentrated bodies of salt water under normal Raman excitation can have visible carotenoid bands if enough microorganisms are present, as is shown in the case of the Black Sea samples from 2018. Spectra from indigenous diatom *Skeletonema* sp. has clear carotenoid bands; C=C stretching mode $\sim 1523\text{ cm}^{-1}$, C-C stretching mode $\sim 1157\text{ cm}^{-1}$ and C-H₃ stretching mode $\sim 1014\text{ cm}^{-1}$ (Fig 6. C). The same bands can be observed in the spectra of the concentrated seawater from the surface and from 10 m depth. Spectra of non-concentrated samples from the same place and time do not have carotenoid bands. Concentrated surface seawater had a higher intensity of carotenoids compared to the spectra from 10 m depth (Fig 6. D). The relative intensity ratio for the Cojocna lakes is

shown with error bars based on the standard deviation from the average of each lake (Fig 6. D).

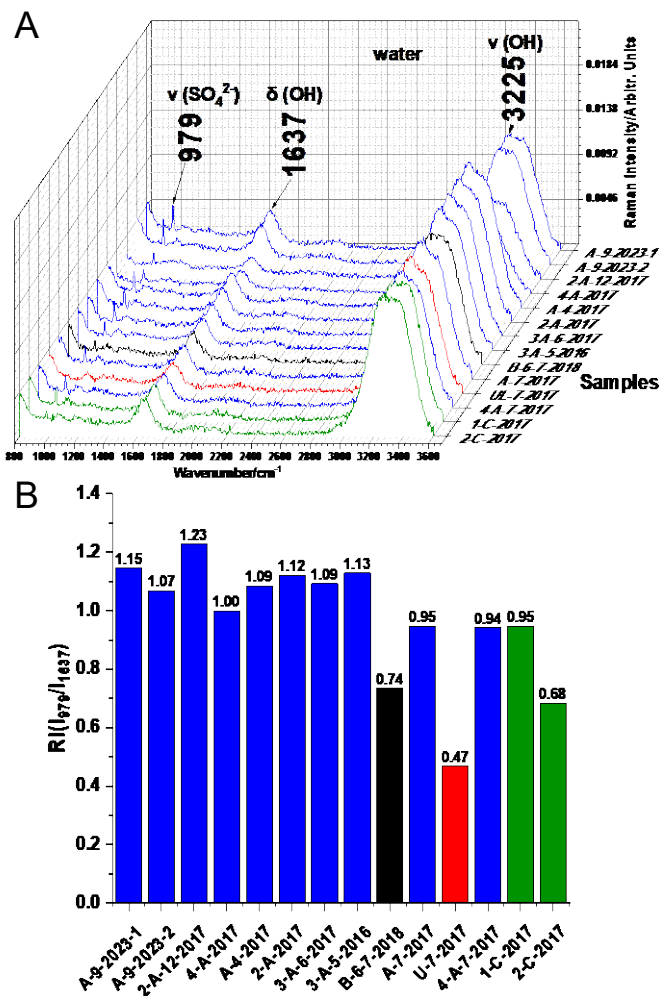


Figure 2. A) 3D-plot of FT-Raman spectra of seawater of 14 samples from different salt water bodies and different time periods; x-axis- wavenumber cm^{-1} , y-axis- Raman intensity in arbitrary units, z-axis- samples. Number before letter-sampling location, A- Adriatic Sea, B- Black Sea, U- Ursu Lake, C- Cojocna lakes. Sulfate stretching band 979 cm^{-1} , water bending 1637 cm^{-1} and stretching 3225 cm^{-1} bands. B) Relative intensity ratio of sulfate stretching band 979 cm^{-1} and water bending band 1637 cm^{-1} ($\text{RI}(I_{979}/I_{1637})$). Color Legend: Blue -Adriatic Sea, black - Black Sea, red - Ursu Lake; green - Cojocna lakes. Number before letter:-sampling location, A- Adriatic Sea, B- Black Sea, U- Ursu Lake, C- Cojocna lakes.

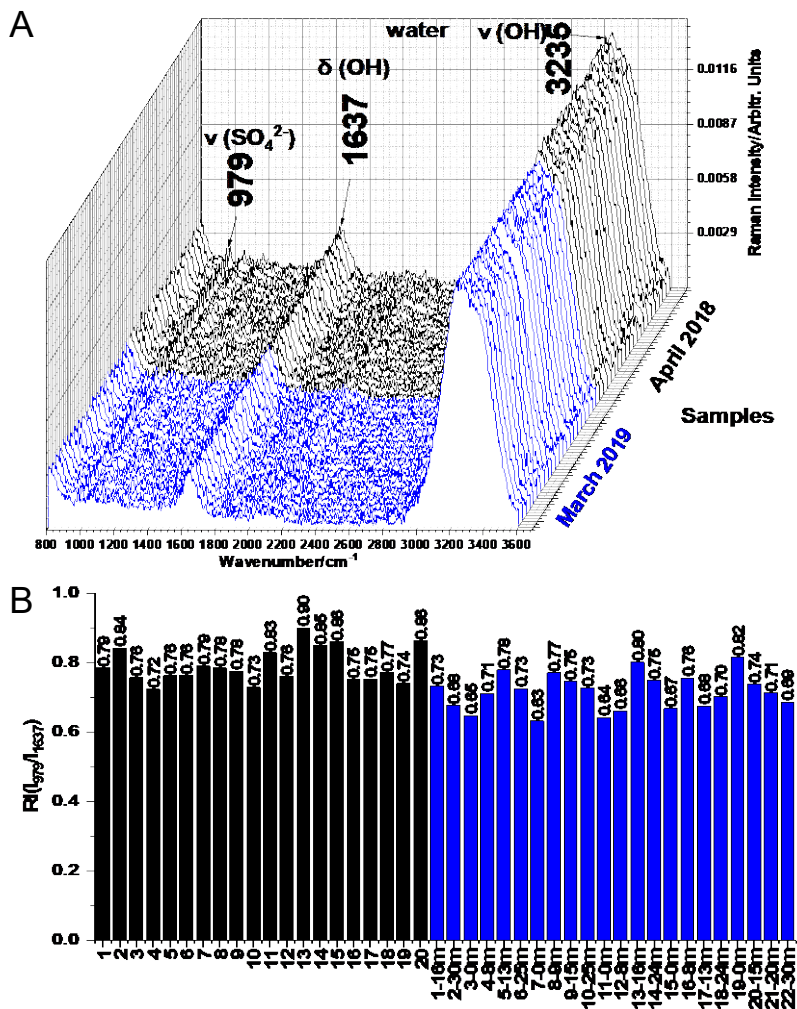


Figure 3. A) 3D-plot of of FT-Raman spectra of seawater (42 samples) from the Black Sea; black colour- 20 samples from **Passarella Mamaia**, April 2018, blue colour- 22 samples at different depth from **Constanța**, March 2019; X-axis- wavenumber(cm^{-1}), y-axis- Raman intensity/ arbitrary units, z-axis- samples from April 2018 and March 2019; Sulfate stretching band at 979 cm^{-1} , water bending at 1637 cm^{-1} and stretching at 3225 cm^{-1} bands.**B**) Relative intensity ratio of sulfate stretching band 979 cm^{-1} and water bending band 1637 cm^{-1} ($\text{RI}(I_{979}/I_{1637})$).

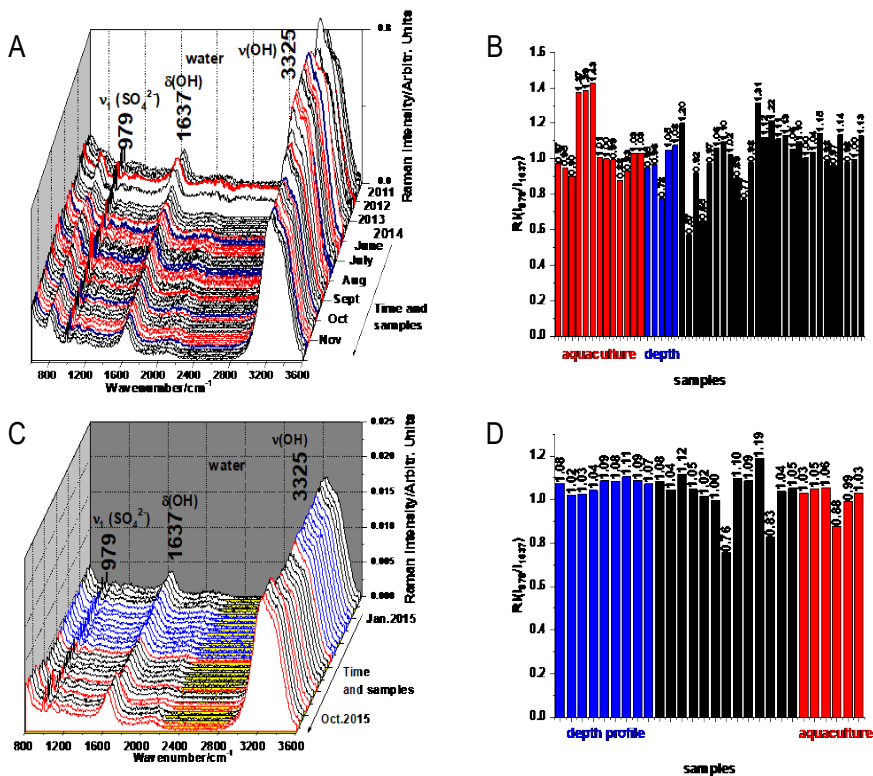


Figure 4. 3D-plot of monthly time dependence of FT-Raman spectra of seawater from the several systematically selected locations for sampling from Adriatic Sea. **A)** 43 samples from 2011, 2012, 2013 and 2014, x-axis- wavenumber (cm^{-1}), y-axis- Raman intensity, z-axis- time and samples; Sulfate stretching band intensity at 979 cm^{-1} is used to calculate the intensity ratio RI (sulfate/water), using the water bending at 1637 cm^{-1} and stretching modes at 3225 cm^{-1} bands, ($\text{RI}(I_{979}/I_{3225})$); Color legend: Red - samples from the **aquaculture area**, blue - **depth samples**. **B)** Relative intensity ratio of sulfate stretching band at 979 cm^{-1} and water bending band at 1637 cm^{-1} ($\text{RI}(I_{979}/I_{1637})$) samples from A); x axis- samples (different locations in the Adriatic Sea): red- **aquaculture area** samples, blue- **depth samples**, y-axis RI. **C)** 28 samples from 2015, x-axis- wavenumber (cm^{-1}), y-axis- Raman intensity/ arbitrary units, z-axis- time and samples; Sulfate stretching band 979 cm^{-1} , water bending 1637 cm^{-1} and stretching 3225 cm^{-1} bands ($\text{RI}(I_{979}/I_{3225})$). Red line- samples from the **aquaculture area**, blue lines- **depth profile** (Feb 2015). **D)** RI of samples from C) x-axis- samples; red- **aquaculture area** samples, blue- **depth samples**, y-axis RI.

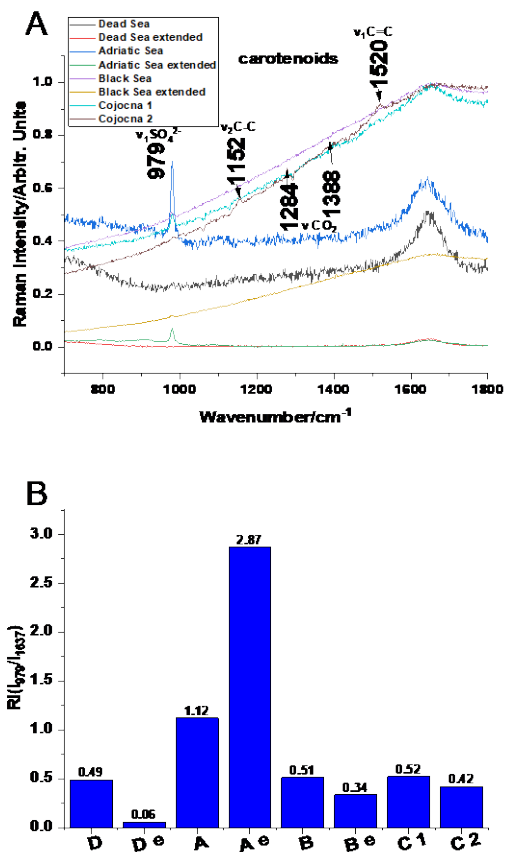


Figure 5. Raw Raman spectra recorded using DCDR from 4 different samples, one Adriatic Sea (autumn 2023), one Black Sea (autumn 2023), one Dead Sea (autumn 2023), and one from each Cojocna lakes (summer 2017). **A)** Adriatic Sea 1 second, 200 mW power, 5x objective; Adriatic Sea extended acquisition 10 min, 200 mW power, 5x objective. Black Sea 30 seconds, 200 mW power, 5x objective; Black Sea extended acquisition 10 min, 200 mW power, 5x objective. Dead Sea, 1 second, 200 mW power, 5x objective; Dead Sea extended acquisition 10 min, 20 mW power, 5x objective. Cojocna Lake 1, 30 seconds, 200 mW power, 5x objective. Cojocna Lake 2 30 seconds, 200 mW power, 5x objective. **B)** Relative intensity ratio of sulfate stretching band 979 cm⁻¹ and water bending band 1637 cm⁻¹ (RI(I₉₇₉/I₁₆₃₇)) for each case.

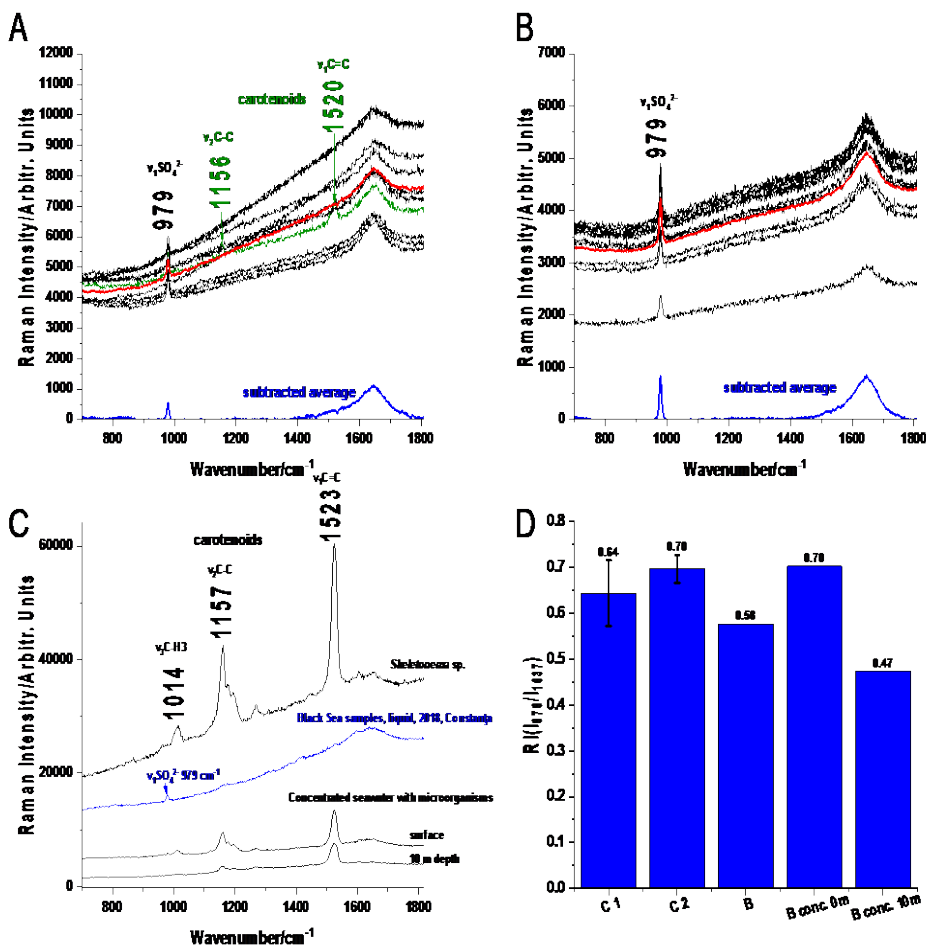


Figure 6. Typical DCDR spectrum from waters rich in microorganisms: two Cojocna lakes (October 2023), **A**), **B**) and Black Sea samples (2018) **A**) Cojocna Lake 1, **B**) Cojocna Lake 2, 5 seconds, 200 mW power. Red line is the **average of 11 measurements** (black lines), blue line- **average subtracted**. In the spectrum was observed the typical bands of **carotenoids** **A**) in one measurement (green line), C=C stretching band ~1520 cm⁻¹ and C-C stretching band 1156 cm⁻¹. **C**) DCDR spectra from the Black Sea samples; blue line- **non-concentrated sample**, bottom two lines- **concentrated seawater samples** with typical carotenoid bands C=C stretching band ~1520 cm⁻¹, C-C stretching band 1156 cm⁻¹ and CH₃ stretching band 1014 cm⁻¹. Reference carotenoid bands from microalgae *Skeletonema sp.* measurements. **D**) Relative intensity ratio of sulfate stretching band at 979 cm⁻¹ and water bending band at 1637 cm⁻¹. For each case C1- Cojocna 1, C2- Cojocna 2, B- Black Sea, B conc. 0m- surface seawater samples from the Black Sea, B conc. 10m seawater sample from 10m depth, Black Sea. Error bars for Cojocna lakes values based on standard deviation from the mean.

4. CONCLUSIONS AND OUTLOOK

Sulfate level in aquatic bodies is easy and fast to measure, due to the existent Raman technology, including portable instruments and is a significant alternative for effective monitoring and quantification based on an adequate calibration curve. Drop-coated deposition of salty bodies of water yields similar results to FT-Raman spectroscopy of bulk waters regarding the relative intensity ratio of sulfate to water bands, which is the basis of an adequate calibration curve for sulfate. Besides sulfate, concentrated drop-coated deposition of salty bodies of water can detect carotenoids, thus, comparatively estimating the microbial population. Further investigation should be made in this direction, opening the possibility for the estimation of carotenoids in waters based on Raman spectroscopy. From these comparative examples discussed in this paper, statistical analysis of spectral data showed significant differences in the relative ratio of sulfate and water bands between the Adriatic Sea and the Black Sea. The mean ratio values of both the Adriatic Sea and the Black Sea are significantly different from the mean ocean value. The comparison of surface samples with depth samples revealed no significant difference in the case for the Black Sea, in contrast for the Adriatic Sea there was a significant difference between ratios proportional with sulfate concentrations. Further, there was a significant difference between the Adriatic Sea ratios in 2014 and 2015. Taking into account everything said, Raman spectroscopy techniques and technologies are prominent tools for water analysis and has potential to be included in monitoring programs.

Sulfate is involved in biogeochemical cycles, including the sulfur cycle (Loka Bharathi, 2008). Understanding the distribution and variations in sulfate concentrations could help understanding natural processes such as microbial sulfate reduction and sulfur oxidation; while changes in sulfate levels may suggest coastal pollution sources, like industrial discharges or other economic activities (Wang and Zhang, 2019). Increased sulfate concentrations may be linked to certain types of pollution. Microbial sulfate reduction is also linked with sulfate level and its monitoring can provide insights into the prevalence of anaerobic conditions, which may impact the types of microbial population (Zavarzin, 2008).

In different registry, sulfate is associated with the seawater corrosivity of metallic structures in marine environments and its monitoring is important for assessing the potential impact on naval and coastal infrastructure (Rajala et al., 2022). In the context of massive concern related to ocean acidification, understanding the chemical composition of seawater, including sulfate concentrations, is crucial for assessing the impacts of changing ocean chemistry. As secondary water quality indicator, sulfate is generally not harmful to human health during touristic and recreational activities at typical concentrations found in seawater, while changes in sulfate levels can influence other water quality parameters, such as pH and alkalinity (Molnár et al., 2023).

REFERENCES

1. Bao, D., Hua, D., Qi, H., Wang, J., 2022. Investigation of a Raman scattering spectral model for seawater containing a composite salt solute. *Opt. Express* 30, 6713. <https://doi.org/10.1364/OE.450250>
2. Fan, Y., Xue, Y., Wang, Y., Liu, R., Zhong, S., 2022. Combined LIBS and Raman spectroscopy: an approach for salinity detection in the field of seawater investigation. *Appl. Opt.* 61, 1718. <https://doi.org/10.1364/AO.451169>

3. Kniggendorf, A.-K., Wetzel, C., Roth, B., 2019. Microplastics Detection in Streaming Tap Water with Raman Spectroscopy. *Sensors* 19, 1839. <https://doi.org/10.3390/s19081839>
4. Kumar, R., Singh, C.K., Kamesh, Misra, S., Singh, B.P., Bhardwaj, A.K., Chandra, K.K., 2024. Water biodiversity: ecosystem services, threats, and conservation, in: *Biodiversity and Bioeconomy*. Elsevier, pp. 347–380. <https://doi.org/10.1016/B978-0-323-95482-2.00016-X>
5. Li, Z., Deen, M., Kumar, S., Selvaganapathy, P., 2014. Raman Spectroscopy for In-Line Water Quality Monitoring—Instrumentation and Potential. *Sensors* 14, 17275–17303. <https://doi.org/10.3390/s140917275>
6. Loka Bharathi, P.A., 2008. Sulfur Cycle, in: *Encyclopedia of Ecology*. Elsevier, pp. 3424–3431. <https://doi.org/10.1016/B978-008045405-4.00761-8>
7. Molnár, C., Drigla, T.D., Barbu-Tudoran, L., Bajama, I., Curean, V., Cîntă Pînzaru, S., 2023. Pilot SERS Monitoring Study of Two Natural Hypersaline Lake Waters from a Balneary Resort during Winter-Months Period. *Biosensors* 14, 19. <https://doi.org/10.3390/bios14010019>
8. Ong, T.T.X., Blanch, E.W., Jones, O.A.H., 2020. Surface Enhanced Raman Spectroscopy in environmental analysis, monitoring and assessment. *Science of The Total Environment* 720, 137601. <https://doi.org/10.1016/j.scitotenv.2020.137601>
9. Rajala, P., Cheng, D.-Q., Rice, S.A., Lauro, F.M., 2022. Sulfate-dependant microbially induced corrosion of mild steel in the deep sea: a 10-year microbiome study. *Microbiome* 10, 4. <https://doi.org/10.1186/s40168-021-01196-6>
10. Shirmohammad, M., Short, M.A., Zeng, H., 2023. A New Gas Analysis Method Based on Single-Beam Excitation Stimulated Raman Scattering in Hollow Core Photonic Crystal Fiber Enhanced Raman Spectroscopy. *Bioengineering* 10, 1161. <https://doi.org/10.3390/bioengineering10101161>
11. Wang, H., Zhang, Q., 2019. Research Advances in Identifying Sulfate Contamination Sources of Water Environment by Using Stable Isotopes. *IJERPH* 16, 1914. <https://doi.org/10.3390/ijerph16111914>
12. Zavarzin, G.A., 2008. Microbial Cycles, in: *Encyclopedia of Ecology*. Elsevier, pp. 129–134. <https://doi.org/10.1016/B978-0-444-63768-0.00745-9>
13. Zhao, J., Lan, R., Wang, Z., Su, W., Song, D., Xue, R., Liu, Z., Liu, X., Dai, Y., Yue, T., Xing, B., 2023. Microplastic fragmentation by rotifers in aquatic ecosystems contributes to global nanoplastic pollution. *Nat. Nanotechnol.* <https://doi.org/10.1038/s41565-023-01534-9>
14. Zhu, G., Li, T., Huang, T., Zhao, K., Tang, W., Wang, R., Lang, X., Shen, B., 2021. Quantifying the Seawater Sulfate Concentration in the Cambrian Ocean. *Front. Earth Sci.* 9, 767857. <https://doi.org/10.3389/feart.2021.767857>